Two-dimensional electron-lattice scattering in thermally oxidized silicon surface-inversion layers

Ching-Yuan Wu and G. Thomas
Department of Electrical Sciences, State University of New York, Stony Brook, New York 11790
(Received 28 June 1973)

Theoretical calculations of the mobility in the thermally oxidized silicon surface-inversion layer for two-dimensional electron-lattice scattering at high surface electric field are presented for the low- and high-temperature cases. It is found that the effective deformation potential associated with lattice scattering of the inversion-layer electron is not necessaily constant for strongly inverted surfaces, i.e., the deformation potential will be surface-electric-field dependent when the electron channel density varies significantly over a lattice constant. In the high-temperature case, it is found that the calculated electron mobility is the same as that calculated by Kawaji if the deformation potential is assumed constant. In the low-temperature high-surface-electric-field case, the electron mobility is proportional to $E_s^{-5/6}$ (assuming the deformation potential to be constant) and $E_s^{-3/2}$ for a simple model of the lattice potential. The calculated results are extended to include different surface orientations and their effect on the occupancy of higher subbands due to the nonequivalence of the valleys. The comparisons of theoretical results with experimental measurements are made.

I. INTRODUCTION

It is well known that the strong surface electric fields associated with the surface inversion layer of an oxidized semiconductor surface can quantize the motion of the carriers in a direction perpendicular to the surface. Shubnikov-de Haas oscillations in a two-dimensional electron gas in the (100) surfaces of a p-type silicon substrate, inverted by an electric field normal to the surface, were first observed by Fowler, Fang, Howard, and Stiles.[1] In their experiment the Shubnikov-de Haas oscillations were observed only at very low temperatures and high gate voltages; at higher temperatures or low surface fields, the quantization may be smeared out by thermal fluctuations of the carriers, scattering of the carriers or inhomogeneities.

Transport properties in the thermally oxidized semiconductors have been extensively studied, both experimentally and theoretically, in recent years.[2-16] Stern and Howard[10] calculated the surface mobility using the model of quantized electrons in a direction normal to the surface and Coulomb scattering of the electrons by charged impurities near the SiO_2-Si interface. This model was particularly successful in explaining experimental observation, especially at low temperatures and moderately strong fields. There have been a number of more detailed and elaborate impurity-scattering calculations in recent years; however, they all contain the same general features: The mobility at low temperature increases with the surface fields in the high-field region. Fang and Fowler[2] point out that, at high temperatures, lattice scattering may be the most important scattering mechanism to intepret their experimental measurement of the temperature dependence of the surface mobility, while surface-impurity scattering might be the dominate scattering mechanism at low surface electric fields. In any event, it seems clear that surface-impurity scattering cannot explain the experimental observation of a rapid decrease in the surface mobility at high surface electric fields. Kawaji proposed a two-dimensional electron-phonon scattering theory to intepret the experimental observations of electron surface concentration, mobility, and its temperature dependence. However, the magnitude of the mobility calculated by Kawaji turned out to be significantly larger than that experimentally measured if the bulk value of deformation potential was used. It has been argued that a change in the magnitude of the deformation potential from the bulk value is physically unjustified. In this paper we show that at very high surface electric field the deformation potential is not a constant and could be larger than the bulk value if the electrons are quantized in a layer only a few lattice constants thick. Some recently published papers[16-19] on the two-dimensional lattice scattering gave essentially the same conclusions for the room-temperature case.

In Sec. II, we will outline the basic equation which describes the scattering of electrons by phonons for the quantized-two-dimensional-gas model. It is shown that the deformation potential for a two-dimensional gas is not a constant but surface-electric-field dependent for very high surface electric field. In Sec. III, we calculate the scattering rate for two-dimensional electron-lattice scattering and then calculate the surface mobility for the high- and low-temperature cases. We then extend the calculations by considering the effect of surface orientation and their effect on the higher subband

occupation due to the nonequivalent valleys with respect to surface orientations. In Sec. IV, the calculated results will be compared to the available experimental data.

II. BASIC EQUATIONS

In the effective-mass approximation, the electronic wave function for the nth subband may be written[10]

$$\phi(x, y, z) = \xi_n(z)\, e^{i\beta z} e^{i(k_x x + k_y y)} \quad , \tag{1}$$

where k_x and k_y are the electron wave vectors in the plane parallel to the SiO_2-Si interface and are measured from the conduction-band edge. β depends only on k_x and k_y and is zero if the effective-mass tensor is diagonal. $\xi_n(z)$ is the envelope wave function that satisfies the equation

$$\frac{d^2\xi_n(z)}{dz^2} + \frac{2m_3^*}{\hbar^2}\left[\mathcal{E}_n + e\phi(z)\right]\xi_n(z) = 0 \quad , \tag{2}$$

where m_3^* is the effective mass perpendicular to the surface and $\phi(z)$ is the surface potential. The boundary conditions that $\xi_n(z)$ must satisfy are $\xi_n(z) = 0$ at $z = 0$ and ∞. If $\phi(z)$ is assumed to be a linear potential[9]

$$\xi_n(z) = K\mathrm{Ai}\left(\alpha(z - z_n)\right) \quad , \tag{3}$$

$$\mathcal{E}_n \simeq (\hbar^2/2m_3)^{1/3}\left[\tfrac{3}{2}\pi e E_s(n + \tfrac{3}{4})\right]^{2/3} \quad , \tag{4}$$

where $\mathrm{Ai}(z)$ is the Airy function, K is the normalization factor and has the value $K = \alpha/\mathrm{Ai}'^2(-\alpha z_n)$, $\alpha = (2m_3^* eE_s/\hbar^2)^{1/3}$, $z_n = \mathcal{E}_n/eE_s$, n is the quantum number, and $\mathcal{E}_n$ is the energy of the quantized electronic subband. The total energy of the wave function $\phi(x, y, z)$ is

$$\mathcal{E}(k) = \frac{\hbar^2 k_x^2}{2m_1^*} + \frac{\hbar^2 k_y^2}{2m_2^*} + \mathcal{E}_n = \frac{\hbar^2 k^2}{2m_{\|}^*} + \mathcal{E}_n \quad , \tag{5}$$

where $m_{\|}^* = (m_1^* m_2^*)^{1/2}$ is the effective mass in the x-y plane.

The total number of electrons in the inversion layer is given by

$$N_{\mathrm{inv}} = (m_{\|}^* n_v/\pi\hbar^2) k_B T \sum_n \ln(1 + e^{(\mathcal{E}_F - \mathcal{E}_n)/k_B T}) , \tag{6}$$

where n_v is the number of equivalent valleys at the surface. The surface electric field is related to the surface charge and the charge of the depletion layer through the equation.

$$N_{\mathrm{inv}} + N_{\mathrm{dep}} = K_s \epsilon_0 E_s/e \quad . \tag{7}$$

Finally, the Fermi energy may be related to the surface field through Eqs. (6) and (7):

$$E_s = \frac{e}{K_s\epsilon_0}\left(N_{\mathrm{dep}} + \frac{m_{\|}^* n_v}{\pi\hbar^2} k_B T \sum_n (1 + e^{(\mathcal{E}_F - \mathcal{E}_n)/k_B T})\right) . \tag{8}$$

We now turn to the subject of the scattering of the conduction electrons by lattice waves. Perhaps the simplest model for electron-phonon interaction is through the "rigid-ion" model.[21] The potential of the perfect crystal is the sum of the ionic potentials, i.e.,

$$v_0(\vec{r}) = \sum_n v(\vec{r} - \vec{l}_n) \quad , \tag{9}$$

where $\vec{r}$ is the point of observation and $\vec{l}_n$ is the nth lattice vector. If the ionic potential is fixed rigidly to the ion, a displacement of the nth ion by an amount $\vec{u}_n$ will produce a potential,

$$v(\vec{r}) = \sum_n v(\vec{r} - \vec{l}_n - \vec{u}_n) \quad . \tag{10}$$

If we write the lattice potential of the vibrating system as the sum of the periodic (perfect-crystal) potential and an aperiodic part we obtain a potential,

$$v(\vec{r}) = v_0(\vec{r}) + v'(\vec{r}) \quad , \tag{11}$$

where

$$v'(\vec{r}) = \sum_n \vec{u}_n \cdot \nabla v(\vec{r} - \vec{l}_n) \tag{12}$$

to first order in the displacement. Using the aperiodic potential as a perturbation, the scattering probability is found to be proportional to the square of the matrix element $(m'\vec{k}'|v'|m, k)$, where

$$(m', \vec{k}'|v'|m, k) = -\sum_n c \int e^{-i\vec{q}\cdot\vec{l}_n} e^{-i\vec{k}'\cdot\vec{x}}\, \xi_{m'}(z) \times \vec{\sigma}\cdot\nabla v(\vec{r} - \vec{l}_n)\, \xi_n(z)\, e^{i\vec{k}\cdot\vec{x}} d^3r \quad , \tag{13}$$

where $\vec{k} = k_x\hat{a}_x + k_y\hat{a}_y$, $\vec{x} = x\hat{a}_x + y\hat{a}_y$, $\vec{q}$ is the wave vector of the lattice wave with polarization $\vec{\sigma}$, and c is a constant. In Eq. (13) we have assumed the effective-mass tensor to be diagonal, i.e., $\beta = 0$. If we assume the origin of the coordinate system to be on the surface of the SiO_2-Si interface and write $\vec{l}_n = \vec{l}_{n\|} + l_{nz}\hat{a}_z$, the matrix element in Eq. (12) may be simplified in the usual way. We first sum over the components of the lattice vector $\vec{l}_n$ which are parallel to the surface, yielding the δ function. That is,

$$(m', k'|v'|m, k) = \sum_{l_{n\|}} e^{i(\vec{k} - \vec{k}' - \vec{q})\cdot\vec{l}_{n\|}} \sum_{l_{nz}} \int_0^\infty dz \int_{\text{unit cell}} d^2x\, e^{i(\vec{k} - \vec{k}')\cdot\vec{x}}\, \xi_{m'}(z)\xi_m(z)\sigma\cdot\nabla v(\mathrm{r} - l_{nz}\hat{a}_z) e^{-iq_z l_{nz}}$$

$$= \Big\{ i\vec{\sigma}\cdot(\vec{k} - \vec{k}')\, c' \sum_{l_{nz}} \int_0^\infty dz\, \xi_{m'}(z)\, \xi_m(z) e^{-iq_z l_{nz}}\, v(\vec{r} - l_{nz}\hat{a}_z) - \sum_{l_{nz}} \int_0^\infty dz$$

$$\times \int_{\text{unit cell}} d^2x\, \xi_{m'}(z)\, \xi_m(z)\, e^{i(q_z l_{nz})}\, \sigma_z \frac{\partial v}{\partial z} \Big\} \delta(\vec{k} - \vec{k}' - \vec{q}_{\|} - \vec{K}_{\|}) \, , \tag{14}$$

where $\vec{K}_{\parallel}$ is the component of the reciprocal-lattice vector parallel to the surface SiO_2-Si interface, and c' is a constant obtained by integrating by parts and evaluating $v(\vec{r})$ at the limits of the unit cell.

Even without knowing in detail the form of $\xi_m(z)$ or $v(\vec{r})$ we can make several observations: (i) Unlike electron-phonon scattering in the bulk, both longitudinal and transverse phonons can participate in the scattering, even in the N process (i.e., $\vec{K}=0$). (ii) Lattice momentum is not conserved in general. (iii) The effective deformation potential is surface-field dependent [i.e., through $\xi_m(z)$ if the summation is over only a few lattice constants]. (iv) There is mixing of the m, m' subbands due to the presence of phonons.

Each of the points listed above could lead to an effective deformation potential larger than the bulk value, which would be obtained when $\xi_n(z)$ extends many lattice constants into the bulk of the semiconductor or for the high-order subbands.

As a specific example we will assume the linear surface potential and the potential $v(\vec{r})$ to be the δ function, i.e.,

$$v(\vec{r}) = \mathcal{E}_0 \delta(x)\delta(y)\delta(z) \quad ,$$

where $\mathcal{E}_0$ is a constant. For a bulk semiconductor this potential gives a matrix element $i\vec{\sigma}\cdot(\vec{k}-\vec{k}')\mathcal{E}_0$, assuming the electronic wave function to be $e^{i\vec{k}\cdot\vec{r}}$. For simplicity, let us evaluate this simple example for the wave vector $\vec{q}$ parallel to $\vec{\sigma}$ and in the x-y plane. Then,

$$\begin{aligned}(m'k'|v'|m,k) &= i\vec{\sigma}\cdot(\vec{k}-\vec{k}')\mathcal{E}_0 \sum_{l_{nz}} \int dz \\ &\times \xi_{m'}(z)\,\xi_m(z)\,\delta(z-l_{nz}) \\ &= i\vec{\sigma}\cdot(\vec{k}-\vec{k}')\,\mathcal{E}_0 \sum_{l_{nz}} \xi_{m'}(l_{nz})\,\xi_m(l_{nz}) \quad . \end{aligned} \tag{15}$$

If ξ_m extends over many lattice constants, the summation over l_{nz} can be converted to an integral and the bulk value of deformation potential will be obtained. In this case only intrasubband scattering is possible. However, if ξ_m extends only over a few lattice constants the bulk value is not obtained. After substitution of Eq. (3) into Eq. (15), we see that the effective deformation potential is proportional to $E_s^{+1/3}$ (i.e., to α) for this mode. A similar calculation for the longitudinal mode normal to the SiO_2-Si interface yields a deformation potential proportional to $E_s^{2/3}$ (i.e., to α^2), for the case where ξ_m extends over only a few lattice constants. While the field dependence of the deformation potential will change with the form or $v(\vec{r})$ and $\xi_m(z)$, it seems reasonable to assume the deformation potential proportional to E_s^p where p is some power to be determined from experiments.

The calculation given above is only intended as an illustration of the effect of the surface electric field on the deformation potential. Not only have we used a crude model for $v(\vec{r})$, but the rigid-ion model itself is unrealistic. However, this model has proved successful in explaining the important features of lattice scattering in the bulk of solids. The exact dependence of the deformation potential on surface field and its magnitude can only be obtained from experimental measurements. We now proceed to evaluate the effect of lattice scattering on the mobility by simply assuming the existence of a deformation potential.

III. QUANTIZED ELECTRON INTERACTION WITH LATTICE WAVE

In this section we assume the conduction electrons to have classical free-electron motion in the x-y plane (parallel to the SiO_2-Si interface) and that the phonon normal to the plane simply causes mixing of the subbands. Even though the lattice wave is a three-dimensional wave, the scattering of the quantized conduction electrons will be confined to two dimensions. We also assume the phonon distribution to be undisturbed by the electron scattering. The scattering rate of two-dimensional electrons may be written in a similar way to the three dimensional case,[21] i.e.,

$$\begin{aligned}\frac{\partial f(\vec{k})}{\partial t} = \frac{2\pi}{\hbar}\sum_q \{ &|(\vec{k}, n_{\vec{q}}+1|v'|\vec{k}+\vec{q}, n_{\vec{q}})|^2 \delta(\mathcal{E}_{\vec{k}}-\mathcal{E}_{\vec{k}+\vec{q}}+\hbar\omega_{\vec{q}}) \\ &\times f(\vec{k}+\vec{q})[1-f(\vec{k})] + |(\vec{k}, n_{\vec{q}}-1|v'|\vec{k}-\vec{q}, n_{\vec{q}})|^2 \\ &\times \delta(\mathcal{E}_{\vec{k}}-\mathcal{E}_{\vec{k}-\vec{q}}-\hbar\omega_{\vec{q}}) f(\vec{k}-\vec{q})[1-f(\vec{k})] \\ &- |(\vec{k}-\vec{q}, n_{\vec{q}}+1|v'|\vec{k}, n_{\vec{q}})|^2 (\mathcal{E}_{\vec{k}-\vec{q}}-\mathcal{E}_{\vec{k}}+\hbar\omega_{\vec{q}}) \\ &\times f(\vec{k})[1-f(\vec{k}-\vec{q})] - |(\vec{k}+\vec{q}, n_{\vec{q}}-1|v'|\vec{k}, n_{\vec{q}})|^2 \\ &\times \delta(\mathcal{E}_{\vec{k}+\vec{q}}-\mathcal{E}_k-\hbar\omega_{\vec{q}}) f(\vec{k})[1-f(\vec{k}+\vec{q})]\} \quad , \end{aligned} \tag{16}$$

where $\vec{k}, \vec{q}$ are the transverse components of the electron wave vector and lattice wave vector, respectively (i.e., the $\parallel$ symbol has been suppressed). The matrix element of electron-lattice scattering can be written in terms of the deformation potential[22]:

$$|(\vec{k}+\vec{q}|v'|\vec{k})|^2 = \frac{\mathcal{E}_1^2\hbar q^2}{2sd\rho_v\omega_q}(n_{\vec{q}}+\tfrac{1}{2}+\tfrac{1}{2}\delta n_{\vec{q}}) \quad , \tag{17}$$

where

$\delta n_{\vec{q}} = -1$ for absorption,

$\delta n_{\vec{q}} = +1$ for emission,

$\mathcal{E}_1$ is the effective deformation potential, ρ_v is the mass density of the semiconductor, s is the surface

area, and d is the width of the layer of lattice atoms with which the electrons can interact. If we assume the scattering to be dominated by acoustic phonons we may write

$$\omega_{\vec{q}} = u_l |\vec{q}| \quad , \tag{18}$$

where u_l is the velocity of sound.

Substitution of Eq. (17) into Eq. (16) yields

$$\frac{\partial f(\vec{k})}{\partial t} = \frac{2\pi}{\hbar} \frac{\mathcal{E}_1^2}{2sd\rho_v u_l^2} \sum_q \hbar\omega_{\vec{q}} \{(n_{\vec{q}}+1)\delta(\mathcal{E}_{\vec{k}} - \mathcal{E}_{\vec{k}+\vec{q}} + \hbar\omega_{\vec{q}}) f(\vec{k}+\vec{q})[1-f(\vec{k})] + n_{\vec{q}}\delta(\mathcal{E}_{\vec{k}} - \mathcal{E}_{\vec{k}-\vec{q}} - \hbar\omega_{\vec{q}}) f(\vec{k}-\vec{q})[1-f(\vec{k})]$$

$$- (n_{\vec{q}}+1)\delta(\mathcal{E}_{\vec{k}-\vec{q}} - \mathcal{E}_{\vec{k}} + \hbar\omega_{\vec{q}}) f(\vec{k})[1-f(\vec{k}-\vec{q})] - n_{\vec{q}}\delta(\mathcal{E}_{\vec{k}+\vec{q}} - \mathcal{E}_{\vec{k}} - \hbar\omega_{\vec{q}}) f(\vec{k})[1-f(\vec{k}+\vec{q})]\} \tag{19}$$

The summation over the two-dimensional lattice wave vector $\vec{q}$ can be transformed into the integral:

$$\sum_{\vec{q}} \rightarrow \int_0^{2\pi} d\theta \int_0^{q'} \frac{S}{(2\pi)^2} q\,dq \quad . \tag{20}$$

The integral

$$I(\vec{k}+\vec{q}) = \int_0^{2\pi} \delta(\mathcal{E}_{\vec{k}} \mathcal{E}_{\vec{k}+\vec{q}} + \hbar\omega_{\vec{q}})\,d\theta \tag{21}$$

may be performed with the aid of the change of variables

$$x = \mathcal{E}_{\vec{k}} - \mathcal{E}_{\vec{k}+\vec{q}} + \hbar\omega_{\vec{q}} = \frac{\hbar^2 k^2}{2m_{\parallel}^*} - \frac{\hbar^2(\vec{k}+\vec{q})^2}{2m_{\parallel}^*} + \hbar\omega_{\vec{q}} \quad ,$$

$$dx = \frac{2\hbar^2 kq}{2m_{\parallel}^*} \sin\theta\, d\theta \quad , \tag{22}$$

where θ is the angle between $\vec{k}$ and $\vec{q}$. Hence,[23]

$$I(\vec{k}+\vec{q}) = 2 \int_{x(\theta=0)}^{x(\theta=\pi)} \delta(x)\, m_{\parallel}^* dx \Big/ \hbar^2 kq \times \left[1 - \left(\frac{m_{\parallel}^*}{\hbar^2 qk}\right)^2 \left(\hbar\omega_{\vec{q}} - \frac{\hbar^2 q^2}{2m_{\parallel}^*} - x\right)^2\right]^{1/2}$$

$$\simeq \frac{2m_{\parallel}^*}{\hbar^2 kq} \left[1 - \left(\frac{q}{2k}\right)^2\right]^{-1/2} \quad . \tag{23}$$

The last approximation is valid as long as $\hbar\omega_{\vec{q}}$ is small, where $\hbar\omega_{\vec{q}}$ is the energy of the acoustic phonon. The calculations of the other δ functions in Eq. (19) also yields the last expression of Eq. (23), provided $\hbar\omega_{\vec{q}}$ is small. Under this condition the scattering rate can be simplified to yield

$$\frac{\partial f(\vec{k})}{\partial t} = \frac{2\pi}{\hbar} \frac{\mathcal{E}_1^2}{2d\rho_v u_l^2} \frac{2}{(2\pi)^2} \frac{m_{\parallel}^* u_l}{\hbar k} \times \int_0^{2k} \{(n_{\vec{q}}+1) f(k+\vec{q})[1-f(\vec{k})] + n_{\vec{q}} f(\vec{k}-\vec{q})[1-f(\vec{k})] - (n_{\vec{q}}+1) f(\vec{k})[1-f(\vec{k}-\vec{q})] - n_{\vec{q}} f(\vec{k})[1-f(\vec{k}+\vec{q})]\} \frac{qdq}{[1-(q/2k)^2]^{1/2}} \quad . \tag{24}$$

Equation (24) is valid at all temperatures if the electrons are quantized to have only two-dimensional free-electron motion. In order to compare with experimental data, it is necessary to obtain an expression for the channel mobility as a function of surface field. We consider two cases:

A. High-temperature case

At high temperatures, the phonon can be assumed to be fully excited, i.e., $n_{\vec{q}} = k_B T/\hbar\omega_{\vec{q}} \gg 1$, and the electron distribution function may be written

$$f(\vec{k}\pm\vec{q}) = f(\mathcal{E}_{\vec{k}} \pm \hbar\omega_{\vec{q}}) \simeq f^0(\mathcal{E}_{\vec{k}}) \pm \hbar\omega_{\vec{q}} \frac{\partial f^0}{\partial \mathcal{E}} \quad . \tag{25}$$

Substitution of Eq. (25) into Eq. (24) yields

$$\frac{\partial f(k)}{\partial t} \simeq \frac{\mathcal{E}_1^2 m_{\parallel}^* k_B T}{\rho_v d u_l^2 \hbar^3} [f(\vec{k}) - f^0(\vec{k})] \quad . \tag{26}$$

Treating the electron motion in the two dimensions to be classical we may immediately write the relaxation time for acoustic-phonon scattering

$$\tau_{ac}^{-1} = \frac{\mathcal{E}_1^2 m_{\parallel}^* k_B T}{\rho_v u_l^2 \hbar^2 d} \quad . \tag{27}$$

The effective mobility in the surface inversion layer then becomes

$$\mu_{eff} = \frac{e\tau_{ac}}{m_{\mu}^*} = \frac{e\rho_v u_l^2 \hbar^3 d}{\mathcal{E}_1^2 m_{\mu}^* m_{\parallel}^* k_B T} \quad , \tag{28}$$

where m_{μ}^* is the conduction-electron effective mass. The expression of mobility given in Eq. (28) is the same[23] as that calculated by Kawaji except that the conduction mass is used to define the effective mobility.

B. Low-temperature case

At sufficiently low temperatures, the phonons that can be excited are quite limited, hence, $1 \gg n_q \simeq 0$. In this case Eq. (24) can be written

$$\frac{\partial f(\vec{k})}{\partial t} = \frac{2m_{\parallel}^* \mathcal{E}_1^2}{4\pi\rho_v d u_l \hbar^2 k} \times \left([1-f(\vec{k})] \int_0^{2k} f(\vec{k}+\vec{q}) \frac{qdq}{[1-(q/2k)^2]^{1/2}} - f(\vec{k}) \int_0^{2k} [1-f(\vec{k}-\vec{q})] \frac{qdq}{[1-(q/2k)^2]^{1/2}}\right) \quad . \tag{29}$$

Further simplification results at high surface fields, $\mathcal{E}_{\vec{k}} \gg \hbar\omega_{\vec{q}}$, which means that $f(\mathcal{E} \pm \hbar\omega_{\vec{q}})$

$\simeq f^0(\mathcal{E}_{\vec{k}})$. Hence, the scattering rate can be approximately by

$$\frac{\partial f(\vec{k})}{\partial t} = \frac{2\mathcal{E}_1^2 m_{\parallel}^* k}{4\pi\rho_v u_l \hbar^2 d}\left[f^0(\vec{k}) - f(\vec{k})\right] \quad . \tag{30}$$

Again, assuming that the electron motion in two dimensions to be classical, the relaxation time can be written

$$\tau_{ac}^{-1} = 2\mathcal{E}_1^2 m_{\parallel}^* k / \pi\rho_v u_l \hbar^2 d \tag{31}$$

and the effective mobility can be written

$$\mu_{eff} = \pi\rho_v e\hbar^2 u_l d / 2\mathcal{E}_1^2 m_{\parallel}^* m_{\mu}^* k_F \quad , \tag{32}$$

where k_F is the two-dimensional wave number evaluated at the Fermi energy.

There remains two variables to the determined in Eq. (32): The width of the channel layer d over which the electron can interact with the lattice waves, and the two-dimensional wave vector k_F. If we assume that at low temperature only the lowest electric subband is occupied, the total electron density per unit area in the inversion layer contained in the lowest electronic subband can be written

$$N_{inv} = \frac{m_{\parallel}^* n_v k_B T}{\pi\hbar^2} \ln\left[1 + \exp\left(\frac{\mathcal{E}_F - \mathcal{E}_n}{k_B T}\right)\right]\Bigg|_{n=0} \quad . \tag{33}$$

For low temperature and high fields, $(\mathcal{E}_F - \mathcal{E}_0)/k_B T \gg 1$ and Eq. (33) becomes

$$N_{inv} \simeq \frac{m_{\parallel}^* n_v}{\pi\hbar^2}(\mathcal{E}_F - \mathcal{E}_0) \quad . \tag{34}$$

Combining Eqs. (34) and (8), we obtain

$$\mathcal{E}_F - \mathcal{E}_0 = \frac{\pi\hbar^2}{m_{\parallel}^* n_v}\frac{K_s\epsilon_0}{e}\left(E_s - \frac{eN_{dep}}{K_s\epsilon_0}\right) \quad . \tag{35}$$

The two-dimensional wave vector k_F can be calculated by using Eqs. (35) and (5) i.e.,

$$k_F = \left[\frac{2\pi K_s\epsilon_0}{en_v} E_s\left(1 - \frac{eN_{dep}}{K_s\epsilon_0 E_s}\right)\right]^{1/2}$$

or

$$k_F = (2\pi/n_v)^{1/2} N_{inv}^{1/2} \quad . \tag{36}$$

It should be noted that mks units are used through out this paper. The width of inversion layer can be calculated in several ways. One method is to use the trial wave function of Howard. The width of inversion layer d can be expressed (mks unit)

$$d = \left(\frac{32}{11}\right)^{1/3}\left(\frac{9K_s\epsilon_0\hbar^2}{4e^2 m_3^*}\right)^{1/3}\left(\tfrac{13}{11}N_{dep} + N_{inv}\right)^{-1/3} \quad , \tag{37}$$

the other is the direct use of the relation $eE_s d = E_0$, the d can be expressed as (mks unit)

$$d = \left(\frac{81\pi^2\hbar^2 K_s\epsilon_0}{128 m_3^* e^2}\right)^{1/3}(N_{inv} + N_{dep})^{-1/3} \quad . \tag{38}$$

The ratio of the coefficients of Eqs. (37) and (38) is about 1.015 75, so the expression in Eq. (37) or Eq. (38) is almost the same for the lowest subband. It has been shown by F. Stern,[20] that the eigenvalues ξ_n in Eq. (4) are amazingly close to the self-consistent results even for the lowest subband. Hence, it is simpler to use Eqs. (4) and (38) rather

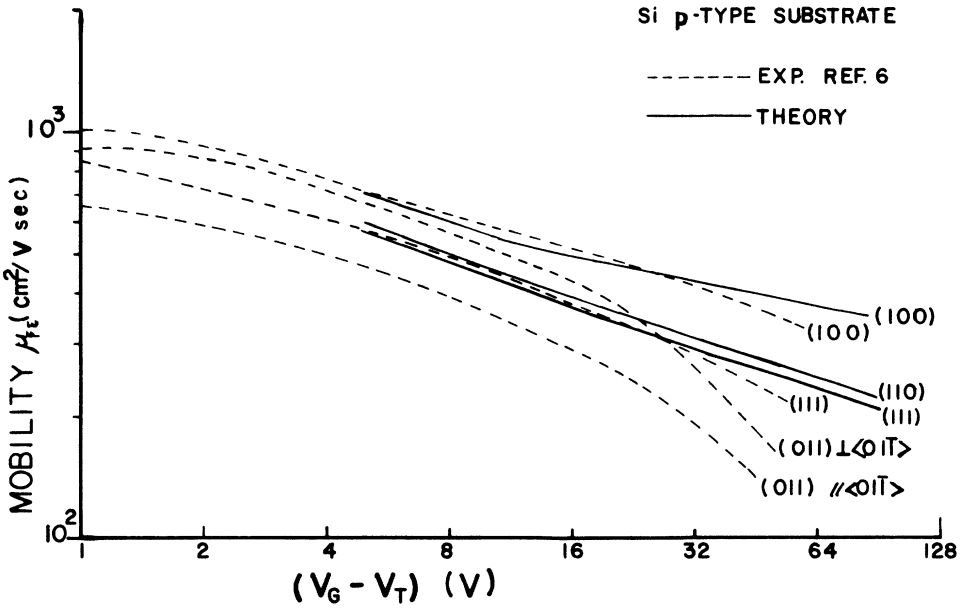

FIG. 1. Theoretical calculations of the field-effect mobility μ_{FE} vs gate voltages ($\log_2$ scale) for the (100), (111), and (110) surfaces with the data from Ref. 6.

than the self-consistent calculations to examine the effort of the higher subband. We will use this method in Sec IV. From Eqs. (36) and (38), the effective mobility for high temperature and the lowest electric subband can be written

$$(\mu_{eff})_H = C_H E_s^{-1/3} T^{-1} \quad , \tag{39}$$

where

$$C_H = \frac{e\pi\rho_v u_l^2 \hbar^3}{\mathcal{E}_1^2 m_\mu^* m_\parallel^* k_B} \left(\frac{81\pi^2\hbar^2}{2m_3^* e}\right)^{1/3} .$$

For the low-temperature case the effective mobility can be written

$$(\mu_{eff})_L = C_L E_s^{-5/6} \quad , \tag{40}$$

where the constant

$$C_L = \frac{\pi\rho_v e u_l \hbar^2}{8\mathcal{E}_1^2 m_\parallel^* m_\mu^*} \left(\frac{81\pi^2\hbar^2}{2m_3^* e}\right)^{1/3} \left(\frac{en_v}{2\pi K_s \epsilon_0}\right)^{1/2} .$$

It is clear that the effective mobility at low temperature and high surface electric field is a steeply decreasing function of surface electric field. Equation (40) predicts the mobility to be independent of temperature. A more rapid decrease in the mobility with respect to surface field is predicted if $\mathcal{E}_1$ increases with surface field as can be expected from the calculation in Sec. II. For example, for the model used in the calculation of Sec. II μ_{eff} would be proportional to $E_s^{-3/2}$ when the surface field is high enough so that the inversion layer width is only a few lattice constants wide.

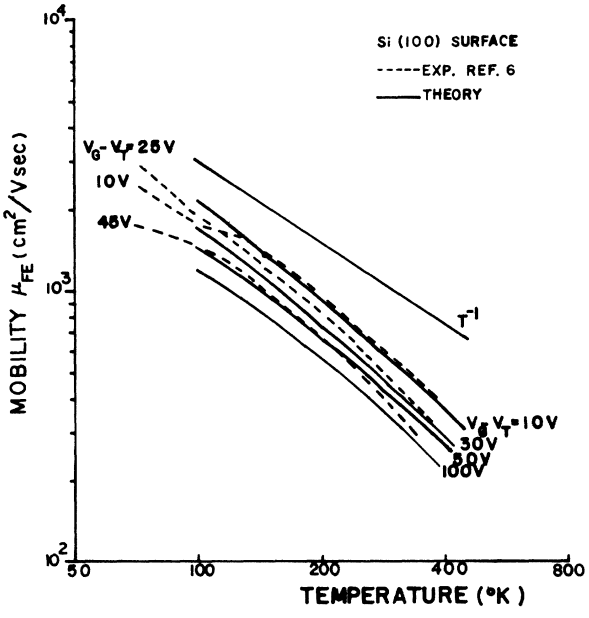

FIG. 2. Theoretical calculations of the field-effect mobility μ_{FE} vs temperature ($\log_2$ scale) for the (100) surface with variable gate voltages, are compared with the data from Ref. 6.

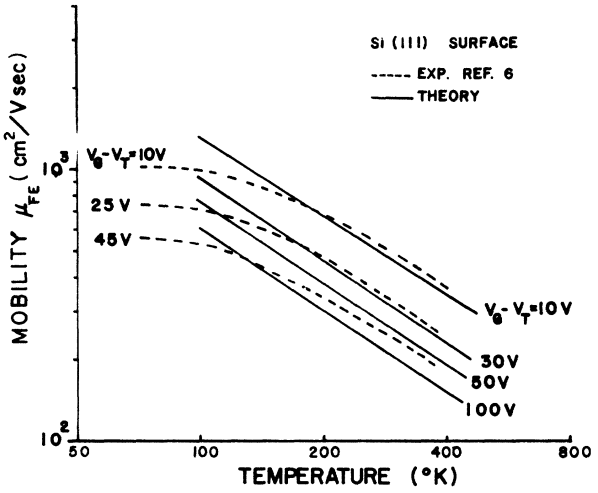

FIG. 3. Theoretical calculations of the field-effect mobility μ_{FE} vs temperature ($\log_2$ scale) for the (111) surface with variable gate voltages, are compared with the data from Ref. 6.

For high temperatures, the calculation of the lowest subband is not enough to predict the behavior of the surface electric field and temperature dependence of surface mobility.

C. Effects of surface orientations and higher subbands

In Sec. III we assumed an isotropic deformation potential constant hence the anisotropy of surface mobility is due to the differences in the effective mass for the difference crystalline directions. For the (111) surface, $m_1^* = m_t^*$, $m_2^* = \frac{1}{3}(m_t^* + 2m_l^*)$, $m_3^* = 3m_t^* m_l^*/(m_t^* + 2m_l^*)$, $m_\parallel^* = (m_1^* m_2^*)^{1/2}$, $m_\mu^* = 2m_1^* m_2^*/(m_1^* + m_2^*)$, and the valley degeneracy n_v is 6. For the (100) surface, the six valleys are not all equivalent; in two of the valleys: $m_\parallel^* = m_t^*$, $m_3^* = m_l^*$, $m_\mu^* = m_t^*$; and for the other four valleys: $m_\parallel^* = (m_t^* m_l^*)^{1/2}$, $m_3^* = m_t^*$, $m_\mu^* = 2m_t^* m_l^*/(m_t^* + m_l^*)$, with the two-valley degeneracy occupying lower subbands than the four-valley degeneracy: For the (110) surface, four valleys have $m_\parallel^* = [\frac{1}{2} m_t^* \times (m_t^* + m_l^*)]^{1/2}$, $m_3^* = 2m_t^* m_l^*/(m_t^* + m_l^*)$, $m_\mu^* = 2m_t^* \times (m_t^* + m_l^*)/(3m_t^* + m_l^*)$, and the other two valleys have $m_\parallel^* = (m_t^* m_l^*)^{1/2}$, $m_3^* = m_t^*$, $m_\mu^* = 2m_t^* m_l^*/(m_t^* + m_l^*)$; in this case, the four-valley degeneracy occupy a lower energy subband than the two-valley degeneracy. If the intersubband scattering can be neglected, the average mobility can be calculated by

$$\mu_{eff} = \sum_{ij} \mu_{ij} (N_{inv})_{ij} \Big/ \sum_{ij} (N_{inv})_{ij} \quad , \tag{41}$$

where μ_{ij} and $(N_{inv})_{ij}$ are the effective mobility and carrier concentration in ith subband with j the valley degeneracy. The separation between electric subband can be easily calculated by using Eq. (4).

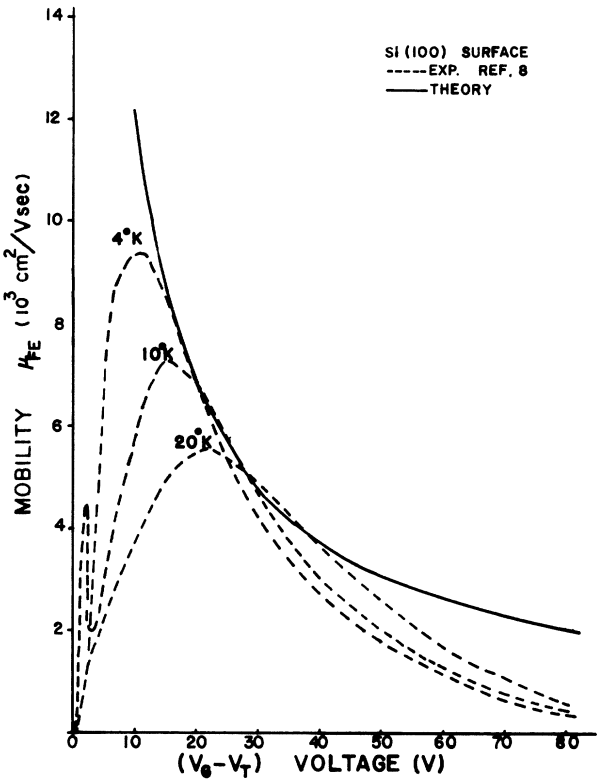

FIG. 4. Theoretical calculations of the field-effect mobility μ_{FE} vs temperature ($\log_2$ scale) for the (110) surface with variable gate voltages are compared with the data from Ref. 6.

For simplicity, we calculate the effect of nonequivalent valley degeneracy in (100), (110), and (111) surfaces. Comparisons between theoretical calculations and experimental data are given in Figs. 1–5. For the (100) surface the effect of the higher subband (which is due to the nonequivalency of valleys) is very important: The deviation from the result of the lowest subband mobility is quite prominant in temperature dependence, magnitude, and carrier concentrations (or surface electric fields); the temperature dependence is stronger than T^{-1} and the carrier concentrations is weaker than $(N_{inv}+N_{dep})^{1/3}$ and the magnitude is smaller than that of lowest subband mobility. For the (110) surface, the total density of states for the higher subband (two valleys) is smaller than the lowest subband (four valleys), so the effect of higher subband is less important than that of the (100) surface, hence the temperature and carrier concentration dependence are only slightly changed. For the low-temperature case, the theoretical calculations predicts the mobility and surface electric field relation to be $\mu_{eff} \propto E_s^{-5/6}$ for the lowest subband in the (100) surface. It should be noted that the relationship between the effective mobility μ_{eff} and field-effect mobility can be written

$$\mu_{FE}(V_G - V_T) \simeq \mu_{eff}(V_G - V_T) + (V_G - V_T)\frac{\partial \mu_{eff}}{\partial V_G} . \tag{42}$$

IV. DISCUSSIONS

From the above theoretical studies, the mobility of the electrons in the inversion layer are calculated in detail for the effects of surface orientation in the (100), and (111) and (110) surfaces and the nonequivalent valley degeneracy is taken into account. We have shown that the inclusion of higher subbands is very important, especially for the (100) surface at higher temperature. Theory predicts that mobility's dependence on field is weaker than $E_s^{-1/3}$ and its temperature dependence is stronger than T^{-1} for (100) surface. For the (111) and (110) surfaces, the mobility can be approximately written as $kE_s^{-1/3}\,T^{-1}$ [only slightly changed for the (110)]. If we use the parameters $m_t^* = 0.19m_0$, $m_l^* = 0.96m_0$; $\rho_v = 2.23\times10^3$ kg/m^3, $\mu_l = 5.4\times10^3$ m/sec, $\mathcal{E}_1 = 9.8$ eV (isotropic deformation potential), the magnitude of mobility is in excellent agreement with the experimental data[6,8] for high-temperature case. From Fig. 1, the experimental data show that the theory predicts less field dependence than experimental data indicates when the gate voltage $(V_G - V_T)$ is above approximately 20 V [equivalent to $(N_{inv}+N_{dep}) = 2\times10^{12}$/cm^2] for all surface orientations. It might be expected that when the gate voltage is larger than 20 V, the mobility's field dependence is stronger than $E_s^{-1/3}$. For low temperature case, Eq. (40) predicts the mobility and surface field relation to be $\mu_{FE} \propto E_s^{-5/6}$ when the inversion layer width d in Eq. (38) is used, the magnitude of μ_{FE} of theoretical calculation is about 2.12

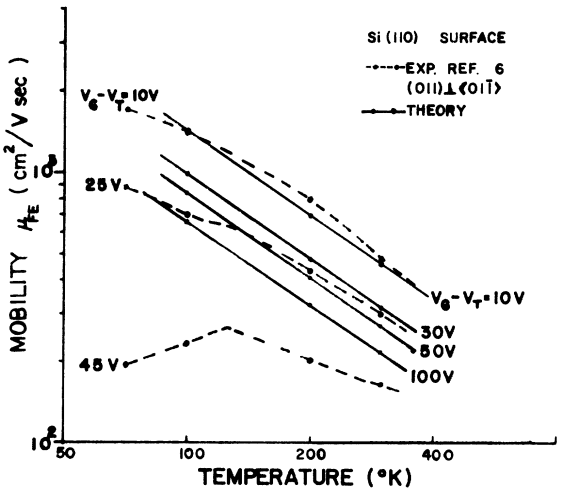

FIG. 5. Theoretical calculations of low-temperature field-effect mobility μ_{FE} vs gate voltage $(V_G - V_T)$ for (100) surface, are compared with the data from Ref. 8.

larger than the experimental data.[8] In Fig. 4, the theoretical calculation is normalized by the above factor to a best fit. The discrepancy can be easily found from the self-consistent calculation of Stern.[20] He shows that at low temperatures the inversion layer width is indeed smaller than that for room temperature by approximately this amount; hence, the magnitude of the discrepancy between the theoretical calculation and experimental data is resolved. From Fig. 4 we clearly see that the same situation happens at low-temperature case: The mobility in the theoretical calculations is less surface-field dependent (or gate voltage) than when the gate $(V_G - V_T)$ is larger than 20 V [equivalent to carrier density $(N_{dep}+N_{inv}) = 8.4\times10^{11}/cm^2$], that is, the mobility has a stronger field dependence than $E_s^{-5/6}$. For low temperatures, the deviation from the shifts in the theoretical calculations to the lower electron densities is as expected, because the inversion layer width is thinner than that at high temperature. In Sec. II, we have shown that when the surface electric field is very high, i.e., the inversion layer width is only several lattice constants, the deformation potential will not be constant and will be surface-electric-field dependent. Any such effect will, of course, be gradual with respect to the surface-electric field, rather than an abrupt change. Another possible way of interpretation may be attributed to surface scattering.[25-27]

The theory developed in this paper predicts a mobility variation E_s^{-n} where $n<1$, yet experimental observations[27] at low temperatures and high fields indicate a variation with $n>1$. An alternative explanation to the one given here (mainly, that that $\mathcal{E}_1$ varies with surface field when the channel thickness is only a few lattice constants thick) has been suggested in Ref. 26. The surface of a semiconductor is never perfectly smooth. Pits in the surface will tend to concentrate the surface field and, hence, squeeze $\xi_n(z)$ closer to the surface. The result will be a channel of nonuniform thickness. It is quite reasonable to assume that such a constriction in the channel thickness would cause scattering. Since the squeezing of the wave function to the surface would be most pronounced at high fields, this scattering mechanism might dominate at high fields. Our suggestion that the deformation potential varies with surface field is only valid if the channel is confined to a few lattice constants in thickness.

It should be noted that the temperature dependence of surface mobility without consideration of the optical-phonon scattering is good enough to interpret the experimental data. In this paper we show that the acoustic lattice scattering is still dominant at low temperatures and high surface fields. If the surface-impurity centers can be reduced, the maximum mobility can be very high (higher than 10 000 cm^2/V sec) and the position of maximum mobility will shift to lower inversion-layer electron concentrations. The theoretical calculations presented are supported by the experimental measurements of N. Kotera *et al.*[8] and F. Fang *et al.*,[2] i.e., the surface state density of N. Kotera *et al.* was of the order of $10^{10}/cm^2$, and the maximum mobility was more than 6800 cm^2/V sec (inversion-layer electron density at maximum mobility was at about $2.1\times10^{11}/cm^2$). The sample of F. Fang *et al.* had a surface-state density of the order of $10^{11}/cm^2$, which gave a maximum mobility of about 5000 cm^2/V sec (inversion-layer electron density was about $5\times10^{12}/cm^2$). Hence, the surface preparation was good, and the maximum mobility tended to be higher and the position of maximum mobility shifts to the lower electron density in the inversion layer, which is yet another piece of evidence tending to confirm that the lattice scattering is still dominant at low temperature and high surface electric fields.

From classical calculations,[15] the effective mobility for very high surface fields at room temperature is $\mu_{eff} \simeq E_s^{-2/5} T^{-1}$ and at low temperatures $\mu_{eff} \propto E_s^{-4/5}$ and independent of temperature.[24] It is surprising that both classical and the quantum models give nearly the same field dependence. Both models show that the effect of increasing the Fermi energy with surface electric field (and hence the increase in the number of electrons interacting with the lattice waves) has a greater effect on the strength of lattice-wave scattering than the decrease in the number of lattice waves excited as temperature decreases. It should be pointed out that the rigid-ion model in Sec. II, is by no means rigorous, and perhaps the effective-mass approximation fails at very high surface electric field, i.e., when the electron wave function is spread over only several lattice constants. However, the model presented tends to predict mobilities which agree with experimental measurements.

[1]A. B. Fowler, F. F. Fang, W. E. Howard, and P. J. Stiles, Phys. Rev. Lett. 16, 901 (1966); J. Phys. Soc. Jap. Suppl. 21, 331 (1966).

[2]F. F. Fang and A. B. Fowler, Phys. Rev. 169, 619 (1968).

[3]F. F. Fang and S. Triebwasser, IBM J. Res. Dev. 8, 410 (1964); Appl. Phys. Lett. 4, 145 (1964).

[4]N. St. J. Murphy, F. Berz, and I. Flinn, Solid State Electron. 12, 775 (1969).

[5]R. F. Pierret and C. T. Sah, Solid State Electron. 11, 279 (1968).

[6]T. Sato, Y. Takeishi, H. Hara, and Y. Okamoto, Phys. Rev. B 4, 1950 (1971).

[7]V. G. K. Reddi, IEEE Trans. Electron Devices, ED-

15, 151 (1968).
[8]N. Kotera, Y. Katayama, I. Yoshida, and K. F. Komatsubara, J. Vac. Sci. and Tech. 9, 754 (1972).
[9]F. Stern, J. Vac. Sci. and Technol. 9, 752 (1972).
[10]F. Stern and W. E. Howard, Phys. Rev. 163, 816 (1967).
[11]E. D. Siggia and P. C. Kwok, Phys. Rev. 2, 1024 (1970).
[12]A. Many, Y. Goldstein, and N. B. Grover, *Semiconductor Surfaces* (North-Holland, Amsterdam, 1965).
[13]J. R. Schrieffer, *Semiconductor Surface Physics*, edited by R. A. Kingston, Univ. of Penn.
[14]S. Kawaji, J. Phys. Soc. Jap. 27, 906 (1969).
[15]C. Y. Wu and G. Thomas, Phys. Rev. B 6, 4581 (1972).
[16]S. Kawaji, H. Ezawa, and K. Nakamura, J. Vac. Sci. Technol. 9, 762 (1972).
[17]H. Ezawa, T. Kuroda, and K. Nakamura, Surf. Sci. 24, 654 (1971).
[18]H. Ezawa, S. Kawaji, and K. Nakamura, Surf. Sci. 27, 218 (1971).
[19]S. Kawaji, H. Ezawa, and K. Nakamura, J. Vac. Sci. Technol. 9, 762 (1972).
[20]F. Stern, Phys. Rev. B 5, 4891 (1972).
[21]For example, see J. Zimon, *Electrons and Phonons* (Cambridge U. P., London, 1964), p. 188.
[22]E. M. Conwell, Solid State Phys. Suppl. 9, 106 (1967).
[23]F. F. Fang (private communication).
[24]C. Y. Wu (unpublished).
[25]Y. C. Cheng and E. A. Sullivan, J. Appl. Phys. 44, 923 (1973).
[26]E. D. Siggia and P. C. Kwok, Phys. Rev. B 2, 1024 (1970).
[27]F. F. Fang and W. E. Howard, Phys. Rev. Lett. 16, 797 (1966).